Available online at www.sciencedirect.com
ScienceDirect
Progress in Natural Science: Materials International 21(2011) 347−354
Progress in Natural Science: Materials International
www.elsevier.com/locate/pnsc

Microstructural evolutions of Cu(Ni)/AuSn/Ni joints during reflow

Xiao-feng WEI, Ri-chu WANG, Chao-qun PENG, Yan FENG, Xue-wei ZHU

School of Materials Science and Engineering, Central South University, Changsha 410083, China

Received 14 March 2011; accepted 23 July 2011

Abstract: Interfacial reactions of the Ni/AuSn/Ni and Cu/AuSn/Ni joints are experimentally studied at 330 °C for various reflow times. The microstructures and mechanical properties of the as-solidified solder joints are examined. The as-solidified solder matrix of Ni/AuSn/Ni presents a typical eutectic ζ'-$(Au,Ni)_5Sn$+δ-(Au,Ni)Sn lamellar microstructure after reflow at 330 °C for 30 s. After reflow for 60 s, a thin and flat $(Ni,Au)_3Sn_2$ intermetallic compound (IMC) layer is formed, and some needle-like $(Ni,Au)_3Sn_2$ phases grow from the IMC layer into the solder matrix. On the other hand, a cellular-type ζ(Cu) layer is found at the upper AuSn/Cu interface in the Cu/AuSn/Ni joint after reflow for 30 s, and a $(Ni,Au,Cu)_3Sn_2$ IMC layer is also formed at the lower AuSn/Ni interface. For both joints the IMC layer grows significantly with the increase of reflow time, but the growth rate of $(Ni,Au,Cu)_3Sn_2$ IMC in the Cu/AuSn/Ni joint is smaller than that of the $(Ni,Au)_3Sn_2$ layer in the Ni/AuSn/Ni joint. The comparisons of the shear strength and fracture surface between the Ni/AuSn/Ni and Cu/AuSn/Ni joints suggest that the coupling effect of the Cu/AuSn/Ni sandwich joint is helpful to prevent the excessive growth of $(Ni,Au)_3Sn_2$, which in turn enhances the mechanical reliability of the solder joint.
Key words: Cu(Ni)/AuSn/Ni joints; interfacial reaction; intermetallic compound (IMC); coupling effect

1 Introduction

Recently, lead (Pb)-free solder has led to extensive research and development to replacing tin-lead (Sn-Pb) solders due to environmental and human health concerns for the Pb toxicity and the ban of Pb usage in electronic products [1−3]. Many alloys, such as Su-Ag, Su-Ag-Cu, and Sn-Zn [4−6], have been proposed as potential Pb-free solders. However, there are somewhat imperfections for these alloys to meet all the requirements for the electronic packaging society and industry today. In response to this situation, the specific electronic packaging using the specific lead-free solder with corresponding design and properties characteristics is the best choice. Eutectic Au-29%Sn (mole fraction) solder is one of the environmentally-friendly lead-free solders and is widely used in the electronics packaging [7−8]. This alloy has excellent anti-fatigue properties and high-temperature performance, superior resistance to corrosion and creep, high electrical and thermal conductivity, in particular, it can be applied through a flux-less bonding process [9−10].

In the electronic products, Cu is the most common conductor metal, which is utilized in contact with solders due to high electrical conductivity, and Ni as a surfacial protection is one of the most common metals to be in direct contact with the solders [11−12]. Therefore, the solder/Cu(Ni) interface is often encountered in optoelectronic products. Many researchers have studied the solder/Cu(Ni) joints to evaluate the reliability of lead-free solder joints [6−7, 13]. Most of the studies were concentrated on single interfacial reactions between solder alloys and metal substrates. However, this type of specimen is far different from the real solder interconnects in electronic packaging, which are usually composed of two different interfaces or metal pads. For this case, the sandwich solder joint specimen can be used to simulate the real solder joint. During the reflow process, the dissolved elements from the metal pads usually have fast diffusions in the molten solder that can quickly diffuse across the molten solder and potentially influence the interfacial reaction on the other side. Especially, Cu and Ni are known to have a high dissolution rate in the Sn-containing solders. As the Sn-containing Pb-free solders start to be implemented in the electronic packaging, the fast diffusion and high dissolution rate of Cu and Ni in the Sn-containing solders will definitely enhance the coupling effect and cause serious reliability issues [14].

In this study, the interfacial reactions of Cu(Ni)/AuSn/Ni sandwich solder joints during reflow at 330 °C

Corresponding author: Ri-chu WANG; Tel: +86-731-88836638; E-mail: wrc910103@163.com

were evaluated. The growth of the intermetallic phases formed at interfaces and the mechanical properties of these solder joints were investigated. In addition, the comparison results between the two systems were reported.

2 Experimental procedures

Au and Sn chips, both of 99.999% purity, were used to prepare the AuSn solder. Proper amounts of Au and Sn chips with dimensions of 20 mm×20 mm×0.1 mm were folded at the sequence of Au/Sn/Au/Sn/Au/Sn/Au, and cold rolled to a mixed metal with a thickness of 0.05 mm, then aged at 245 °C for 14 h to an alloyed AuSn solder. Figure 1 presents the cross-sectional image of AuSn solder. The AuSn solder was cut into lots of small pieces with dimensions of 5 mm×5 mm×0.05 mm. The polished Cu and Ni pads were used as the substrates. A lap shear solder joint was prepared in the specimen as shown in Fig. 2. Reflow reactions were performed as the Cu and Ni pads with the solder pieces were placed in a furnace at 330 °C for 30 s, 60 s, 90 s and 5 min.

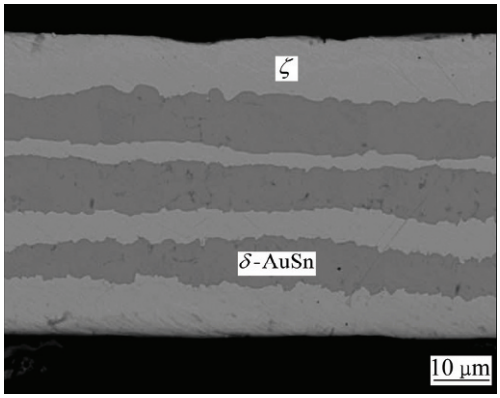

Fig. 1 Cross-sectional image of AuSn solder

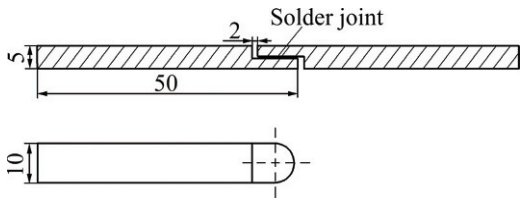

Fig. 2 Specimen of lap shear test solder joint (unit: mm)

After the predetermined reflow time, the furnace power was turned off and the samples were cooled down to room temperature in the water cooled zone of the furnace. The shear test was performed on a Micro Tension Tester. Subsequently, the samples were prepared by common metallographic practices for observations of the interface cross-sections. The microstructure formed at the interface was observed with scanning electron microscope (SEM) equipped. Energy dispersive X-ray (EDX) spectroscopy was used for the compositions analyses. For each compositional analysis, least three measurements were performed and the average values were reported.

3 Results and discussion

3.1 Ni/AuSn/Ni joint

Figure 3 shows the cross-sectional SEM images of the Ni/AuSn/Ni joint reflowed at 330 °C for various times. The AuSn solder matrix presents a two-phase, lamellar eutectic microstructure after reflow for 30 s. The EDX analysis reveals that the compositions in mole fraction of the bright and dark phases are 81.82%Au-15.61%Sn-2.57%Ni and 48.89%Au-47.51%-3.61%Ni, respectively. Based on the Au-Sn binary phase diagram in Fig. 4 [15], the AuSn solder features two kinds of eutectic compositions: Au-29%Sn and Au-93.7%Sn. The Au-29%Sn solder should present a eutectic (ζ'-Au_5Sn+δ-AuSn) microstructure at room temperature. Therefore, it is likely that the bright phase is the ζ'-Au_5Sn and the dark phase is the δ-AuSn, and both of them contain some Ni solubility. These two phases are denoted as ζ'-$(Au,Ni)_5Sn$ and δ-(Au,Ni)Sn in order to show the Ni participation. According to the isothermal section of the Au-Ni-Sn ternary system at room temperature [16], some binary phases in the system such as Au_5Sn, AuSn and Ni_3Sn_2 are known to have a high solubility for the third element, due to the similarity of chemical and physical properties between Au and Ni. It seems that Ni can enter the Au_5Sn and AuSn lattice and substitute for the Au atoms, resulting in the formation of the $(Au,Ni)_5Sn$ and (Au,Ni)Sn phases. It can also be found that there were some coarsened δ-(Au,Ni)Sn phase at the AuSn/Ni interface with a significant Ni solubility based on the analysis result (45.84%Au-46.68%Sn-7.49% Ni).

After reflow for 60 s, the fine lamellar microstructure coarsens significantly, as shown in Fig. 3(b). In addition, a new IMC layer is observed at both the AuSn/Ni interfaces and a needle-like phase grows from the IMC layer into the solder matrix. EDX analysis reveals that the composition in mole fraction of the IMC layer is 14.35%Au-41.19%Sn-44.46%Ni, which is similar to that of the needle-like phase. The ratio of the atomic percentage of (Ni+Au) to that of Sn is 58.81:41.19, which is close to 3:2, suggesting that the reaction product is $(Ni,Au)_3Sn_2$ IMC. The result is consistent with that of LAURILA et al [17] of the Ni-Sn system; they reported that at 300 °C only the Ni_3Sn_2 phase appeared as a layer with thin, long, columnar grains under the reaction condition of Ni excess. In general, the first stage of the reaction in the AuSn/Ni joint is the dissolution of Ni to liquid solder, until the solder is supersaturated with Ni more or less uniformly at the AuSn/Ni interface, Ni_3Sn_2 nucleates and starts to

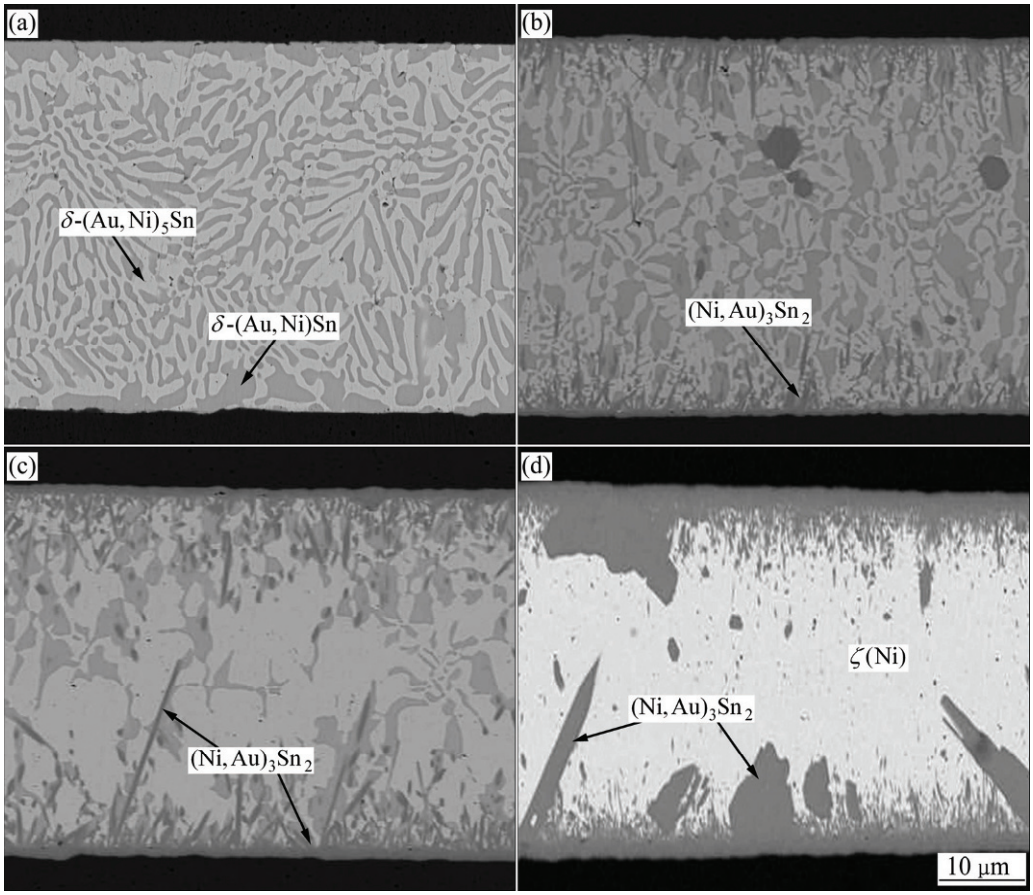

Fig. 3 SEM images of cross-sectional microstructure of Ni/AuSn/Ni solder joints reflowed at 330 °C for various times: (a) 30 s; (b) 60 s; (c) 90 s; (d) 5 min

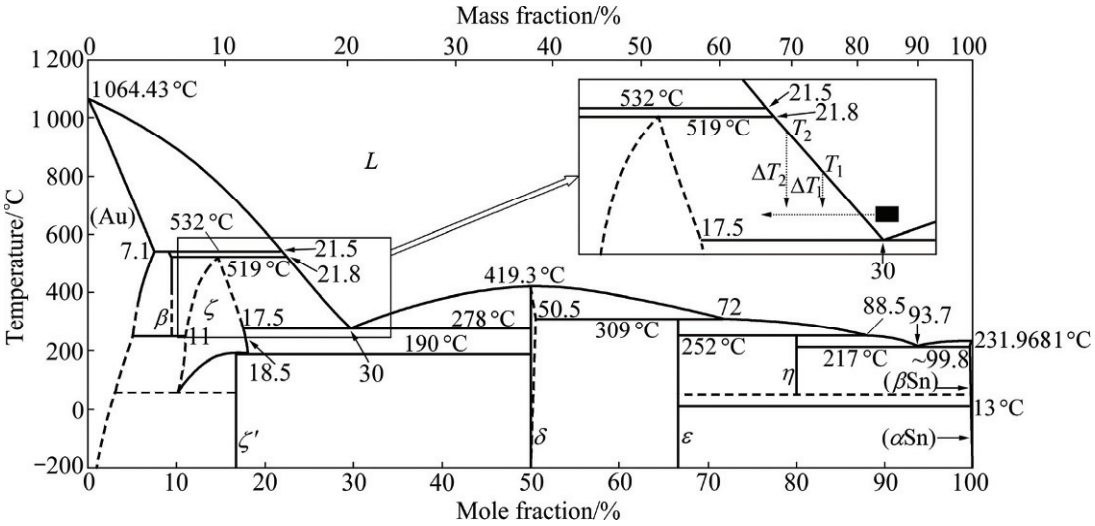

Fig. 4 Au-Sn binary phase diagram [15]

grow. As mentioned before, the Ni_3Sn_2 has a very high solubility for the Au element, resulting in the formation of the $(Ni,Au)_3Sn_2$ IMC layer at the interface. Upon increasing the reflow time, the IMC layer and the needle-like $(Ni,Au)_3Sn_2$ phase grow significantly, as shown in Fig. 3(c).

To evaluate the interfacial reaction of AuSn/Ni joint in longer reflow process, we reflowed the Ni/AuSn/Ni joint at 330 °C for 5 min. It can be found that the eutectic ζ'-$(Au,Ni)_5Sn$+δ-(Au,Ni)Sn microstructure formed when the initial reflow vanished completely. The solder matrix transforms into a ζ(Ni) solid solution, as shown in

Fig. 3(d). Since the interfacial $(Ni,Au)_3Sn_2$ IMC layer grows with the preferential consumption of the available [Sn] in the solder matrix, the composition of the solder matrix shifts into the Au-rich ζ phase region, resulting in the full transformation of the Au-Sn solder into ζ(Ni) phase. In addition, the interfacial $(Ni,Au)_3Sn_2$ phase grew irregularly after reflow for 5 min. The needle-like phase grew in width, and some of them grew together to form a very coarsen phase, as shown in Fig. 3(d). It is well known that the presence of the IMC between solder and conductor metals is an indication of good bonding. However, due to their inherent brittle nature and tendency to generate structural defects, too thick IMC layer at the solder/conductor metal interface may degrade the reliability of the solder joints.

To evaluate the correlation between the micro-structure and mechanical properties of AuSn/Ni joints, we investigated the shear strength of the joints as a function of the reflow time. Figure 5 shows the shear strength values for Ni/AuSn/Ni joints with various reflow times. It was observed that the shear strength of the Ni/AuSn/Ni joints increases slightly with the increase of reflow time to 90 s. Upon increasing to 5 min, however, the shear strength goes down again. To analyze this phenomenon based on the microstructure and fracture surface (as shown in Fig. 6) of the Ni/AuSn/Ni joints, it is clear that it is necessary to form an IMC layer for the bonding between the AuSn solder and Ni substrate. However, the excessive growth of the IMC layer may adversely affect the reliability of solder joints. They become sources of mechanical weakness in the solder joints due to the brittle nature of the intermetallics or cause delamination at the interface. Thus, the excessive growth of the $(Ni,Au)_3Sn_2$ IMC layer should be controlled, which is harmful for the reliability of the solder joint. The results imply that the reflow time must be determined at that case to form the desired IMCs at the interfaces.

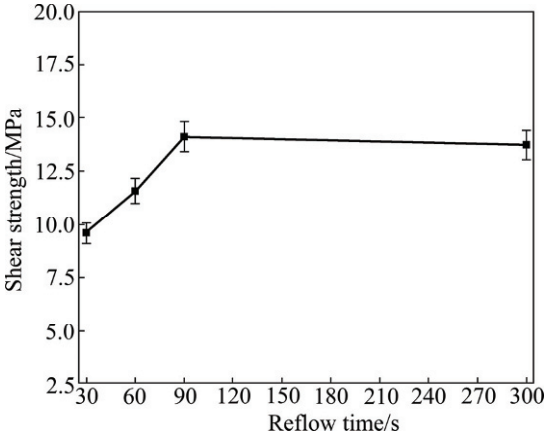

Fig. 5 Shear strength of Ni/AuSn/Ni joints reflowed at 330 °C for various times

3.2 Cu/AuSn/Ni joint

Figure 7 shows the cross-sectional SEM images of the Cu/AuSn/Ni solder joint reflowed at 330 °C for various times. It is observed that the microstructures of the Cu/AuSn/Ni joints are far different from those of the Ni/AuSn/Ni joints. The first different phenomenon is the cellular-type bright phase formed at the upper AuSn/Cu interface after reflow for 30 s. The EDX analysis reveals that the composition in mole fraction of the phase is 71.01%Au-13.7%Sn-15.29%Cu, suggesting that it was also the ζ phase with a significant Cu solubility, denoted as ζ(Cu) solid solution. The above results are consistent with the previous study [7]. During the reflow, the Cu atoms from the Cu substrate continuously dissolve into the molten solder. Since Cu acts chemically like Au, the Sn composition in the molten solder will decrease with the Cu dissolution, and the solder composition will shift toward the Au-rich side, as depicted by the dotted horizontal arrow in the Au-Sn binary phase diagram in Fig. 4. When the solder composition enters into the two-phase ($L+\zeta$) region, the primary ζ phase precipitates and forms as the layer ζ(Cu) layer along the AuSn/Cu interface, as shown in Fig. 6(a). When the sample starts to cool down, more ζ phase will precipitate and grow on the existing ζ phase at the AuSn/Cu interface. Since the composition shift of solder simultaneously creates a supercooling of ΔT_1 below the corresponding equilibrium liquidus (solidification) temperature T_1 of the new hypo-eutectic composition, it will provide a driving force for the cellular growth of the ζ(Cu) phase during solidification. Therefore, pillar-type growth of ζ(Cu) is observed.

The above discussion also explains the irregular growth of the ζ(Cu) phase in the solder matrix. Figure 7 presents the SEM images showing the whole solder joint for clear observation of the ζ(Cu) phase growth. It is clear that in the initial reflow the ζ(Cu) phase is observed only at the upper AuSn/Cu interface, none is in the two-type microstructure of as-solidified solder matrix. After reflow for 60 s, coarsened ζ(Cu) phase is formed in the solder matrix, and much of them have developed tertiary arms, as shown in Fig. 7(b). Upon increasing the reflow time, the ζ(Cu) grows rapidly, and finally completely consumes the two-type microstructure, as shown in Figs. 7(c) and (d). As mentioned before, the composition shift of solder creates a supercooling of ΔT_1. Suppose that this is the case for the initial reflow. Upon increasing the reflow time, the composition shift will be more significant with the Cu dissolution. As a result, the supercooling for the joints of longer reflow time increases as marked by ΔT_2, which leads to the formation of irregular growth of ζ(Cu) phase.

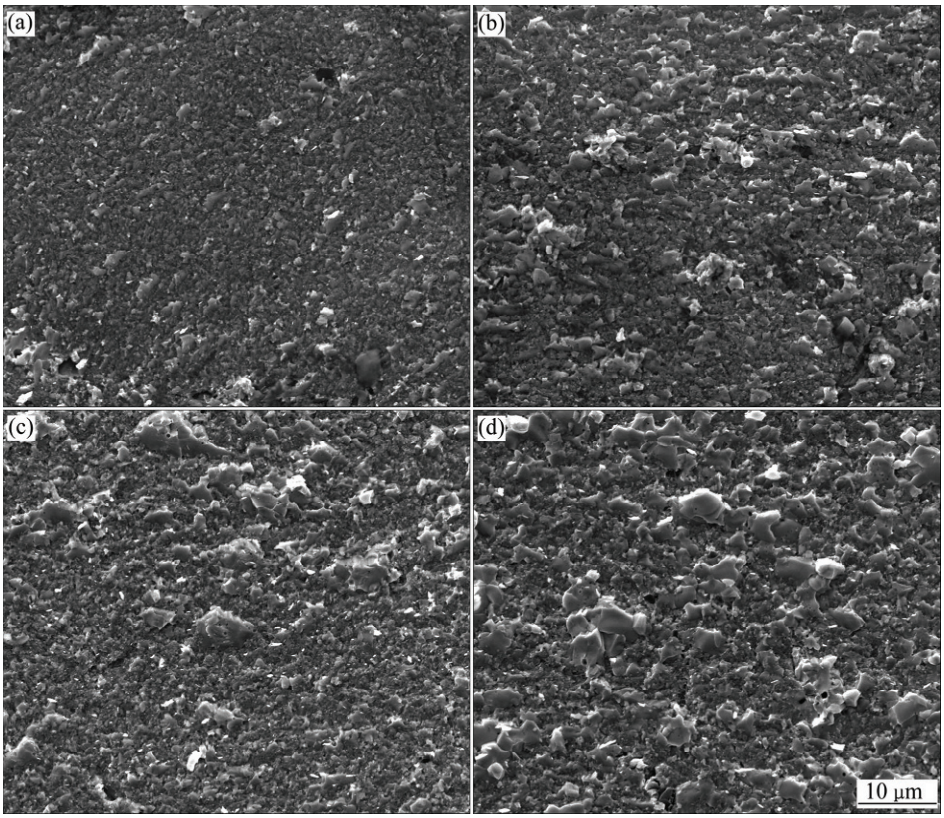

Fig. 6 Top views of fracture surfaces of Ni/Au20Sn/Ni joints reflowed at 330 °C for various times: (a) 30 s; (b) 60 s; (c) 90 s; (d) 5 min

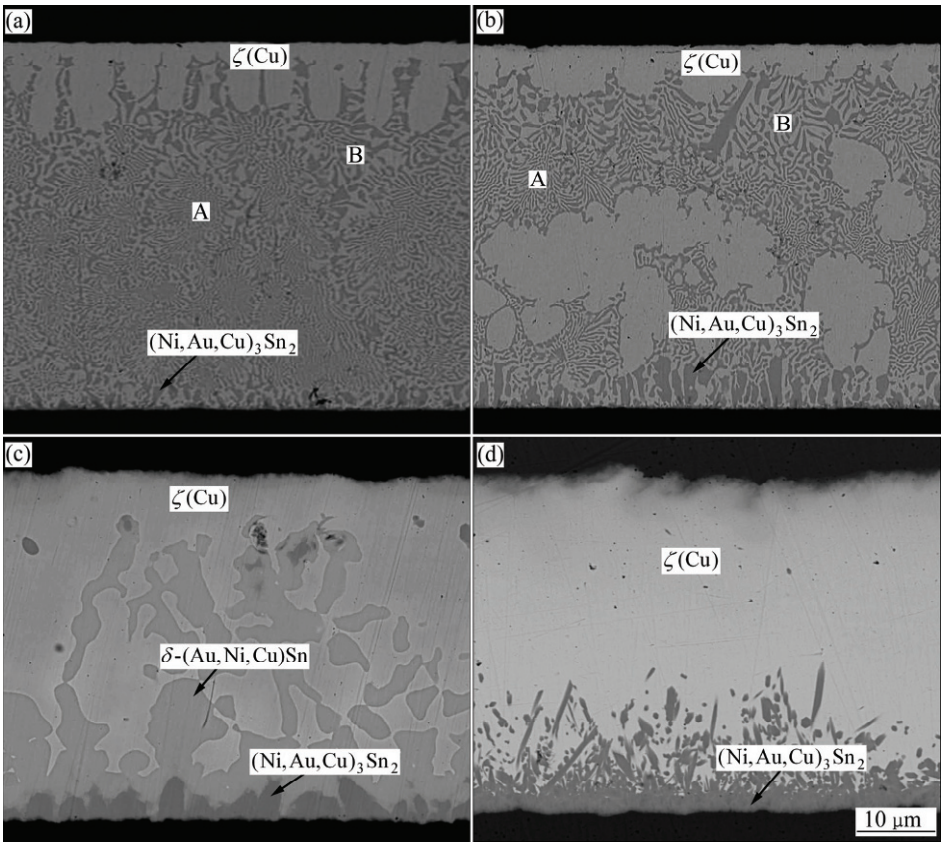

Fig. 7 SEM images of cross-sectional microstructure of Cu/AuSn/Ni solder joint reflowed at 330 °C for various times: (a) 30 s; (b) 60 s; (c) 90 s; (d) 5 min

Another different phenomenon is the evolution of the eutectic microstructure in the solder matrix after reflows for 30 s and 60 s. Two types of eutectic microstructures can be found in the solder matrix; one is fine lamellar microstructure (denoted as A), and the other is coarse microstructure (denoted as B), as shown in Figs. 7(a) and (b). It can also be found that the coarse microstructure is mainly at the Cu side. The EDX analysis shows that both the microstructures are (ζ-Au_5Sn+δ-AuSn) with some Cu and Ni solubility. Upon increasing the reflow time, the amount of the fine lamellar microstructure decreases but that of the coarse microstructure increases. According to CHUNG et al [7], this phenomenon can be explained by the precipitation sequence of ζ+δ phase. Consistent with the above discussion based on the Au-Sn binary phase diagram, the Cu dissolution into the molten solder causes the precipitation of the primary ζ phase. The phases that form during the solidification should be in the sequence of L+ζ→L+ζ+δ→ζ+δ. During the solidification, the molten solder passes through the L+ζ region first, and the primary ζ precipitates grow in the form of pillar. Then the molten solder enters into the L+ζ+δ region where both ζ and δ phases solidify simultaneously. Finally, the remaining liquid transforms into eutectic ζ+δ mixture when entering into the ζ+δ region. This transformation is a typical eutectic reaction and a fine lamellar microstructure is observed, as seen in region A in Figs. 7(a) and (b). In addition, it can be found that a ζ+δ mixture has formed prior to the eutectic reaction as L+ζ→L+ζ+δ. This earlier transformation can also produce a eutectic ζ+δ microstructure. Since both ζ and δ phases will grow continuously during the subsequent cooling, a coarse microstructure is observed, as seen in region B in Figs. 7(a) and (b). Therefore, the as-solidified solder matrix presents a composite microstructure of fine lamellar eutectic and coarse eutectic.

There is also an IMC layer formed at the lower AuSn/Ni interface in the Cu/AuSn/Ni joint. The EDX analysis reveals that the composition in mole fraction of the IMC layer is 42.20%Ni-14.00%Au-3.04%Cu-40.76%Sn. The ratio of the atomic percentage of (Ni+Au+Cu) to that of Sn is 59.24:40.76, which is close to 3:2, suggesting that the reaction product is $(Ni,Au,Cu)_3Sn_2$ IMC. Compared with the IMC formed at the upper interface, we can found that the Cu-Sn IMC at the Cu/AuSn interface contains little Ni solution, but the Ni-Sn IMC contains some Cu solution. It is well known that the dissolution rate of Cu into the molten AuSn solder is much faster than that of Ni [18]. During the reflow, the Cu atoms diffuse rapidly into the solder matrix, and reach the Ni side to participate in the reaction, create a coupling effect on the AuSn/Ni interface. With the increase of the reflow time, the $(Ni,Au,Cu)_3Sn_2$ IMC layer thickens. The growth rate of the $(Ni,Au,Cu)_3Sn_2$ IMC layer in the Cu/AuSn/Ni joint is much slower than that of the $(Ni,Au)_3Sn_2$ IMC layer in the Ni/AuSn/Ni joint. Upon increasing the reflow time to 5 min, the $(Ni,Au,Cu)_3Sn_2$ IMC layer is uniform and regular sized, as shown in Fig. 7(d). This suggests that the coupling effect of the Cu at the upper interface of Cu/AuSn/Ni solder joint is helpful to prevent the excessive growth of the $(Ni,Au,Cu)_3Sn_2$ IMC.

The lap shear test was also performed to evaluate the effect of the microstructure on the mechanical reliability of the Cu/AuSn/Ni solder joints as a function of reflow times. Figure 8 shows the shear strength of Cu/AuSn/Ni joints for various reflow times. As a whole, the shear strength value does not change much as a function of the reflow time, although the strength slightly increases after reflow for up to 5 min. The mean shear strength is 16.5−20.1 MPa in this study. After the lap shear tests, metallurgical observations of the fracture surfaces were performed by SEM. Figure 9 shows the top views of the fracture surface for the Cu/AuSn/Ni joints reflowed at 330 °C for various reaction times. Regardless of different reflow times, the fracture always occurs at the interface of solder/Ni substrate as shown in Fig. 9. The $(Ni,Au,Cu)_3Sn_2$ IMC, formed at the interface, is observed on the fracture surface. Generally, in the lap shear test, a fracture occurs at the interface with the lowest strength. In Cu/AuSn/Ni joints, the ζ(Cu) solid solution is formed at the upper Cu/AuSn interface, of which the bonding strength and plasticity are better than that between the brittle IMC and the solder matrix. Therefore, the fracture of the Cu/AuSn/Ni joints occurs at the solder/Ni interface.

Compared with the shear strength of the Ni/AuSn/

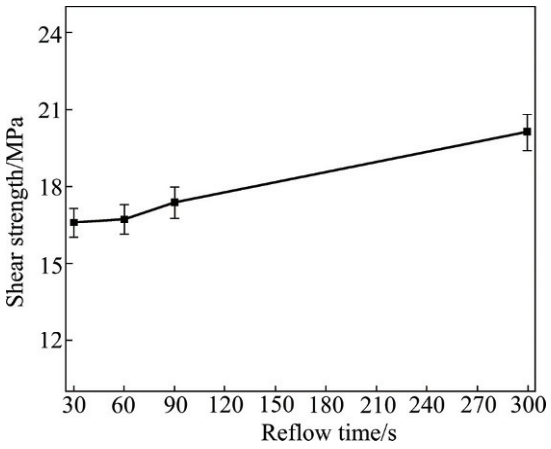

Fig. 8 Shear strength of Cu/AuSn/Ni joints reflowed at 330 °C for various times

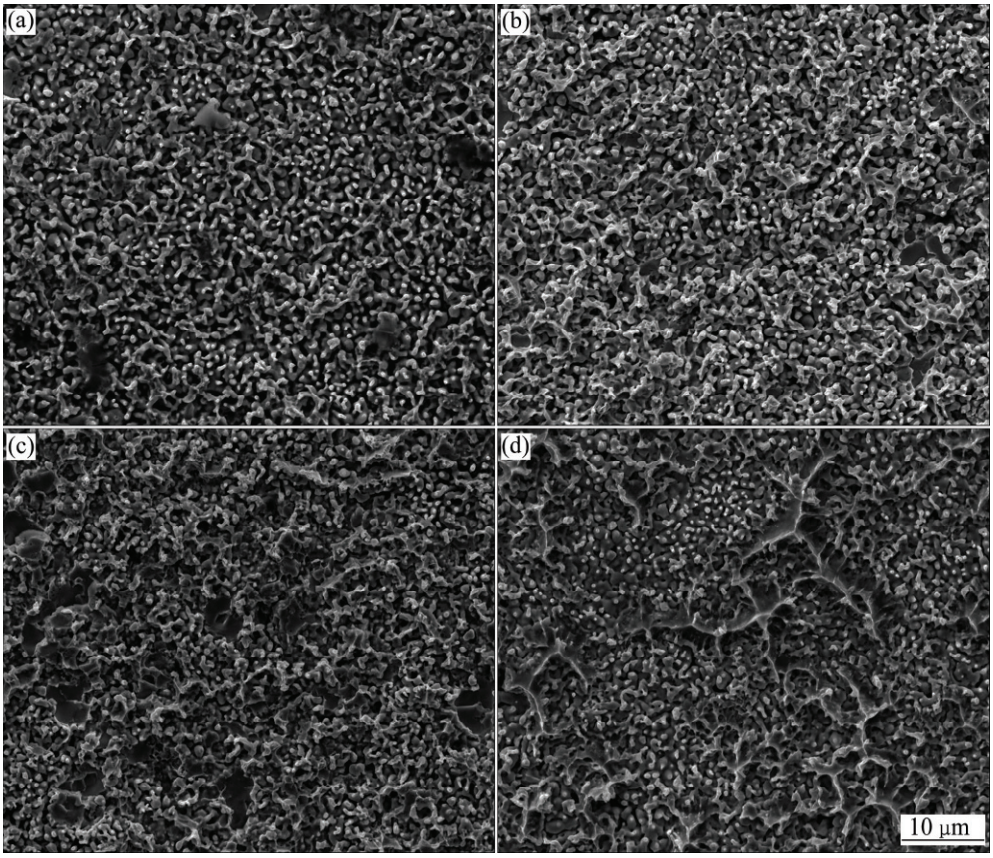

Fig. 9 Top views of fracture surfaces of Cu/Au20Sn/Ni joints reflowed at 330 °C for various times: (a) 30 s; (b) 60 s; (c) 90 s; (d) 5 min

Ni joints shown in Fig. 5, we can find that the shear strength of the Cu/AuSn/Ni is higher. This indicates that the coupling effect of the Cu/AuSn/Ni sandwich joint enhances the mechanical reliability of the solder joint.

4 Conclusions

1) After reflow for 30 s, the Ni/AuSn/Ni solder joint presents a eutectic ζ-$(Au,Ni)_5Sn$+δ-(Au,Ni)Sn lamellar microstructure. The needle-like $(Ni,Au)_3Sn_2$ phase is formed and grows in the solder matrix when the reflow time is prolonged. This is attributed to the Ni dissolution from the Ni substrate into the molten solder matrix. After the solder matrix has been supersaturated with Ni more or less uniformly at the AuSn/Ni interface, $(Ni,Au)_3Sn_2$ nucleates and starts to grow. After reflow for 5 min, the $(Ni,Au)_3Sn_2$ grows irregularly.

2) The microstructure of the Cu/AuSn/Ni joint is far different from that of the Ni/AuSn/Ni joint. The ζ(Cu) layer is formed at the upper AuSn/Cu interface approximately in the form of pillar after reflow for 30 s. It grows irregularly in the solder matrix with the prolonging reflow time due to the driving force of the supercooling, which is caused by the shift of the solder composition. A $(Ni,Au,Cu)_3Sn_2$ layer is formed at the lower AuSn/Ni interface, and thickens with the increase of the reflow time, But the growth rate is much slower than that the $(Ni,Au)_3Sn_2$ layer in the Ni/AuSn/Ni joints. This suggests that the coupling effect of Cu at the upper interface of Cu/AuSn/Ni solder joint is helpful to prevent the excessive growth of the $(Ni,Au,Cu)_3Sn_2$ IMC.

3) The comparison of the shear strength between the Ni/AuSn/Ni and Cu/AuSn/Ni joints indicates that the coupling effect of the Cu/AuSn/Ni sandwich joint enhances the mechanical reliability of the solder joint.

References

[1] CHEN C H, LIN C P, CHEN C M. Effect of Cu thickness on the evolution of the reaction products at the Sn-9wt.%Zn solder/Cu interface during reflow [J]. Journal of Electronic Materials, 2009, 38(1): 61−69.

[2] CHEN C M, CHEN C H, LIN C P, et al. Morphological evolution of the reaction product at the Sn-9wt.%Zn/thin-film Cu interface [J]. Journal of Electronic Materials, 2008, 37(10): 1605−1610.

[3] MOOKAM N, KANLAYASIRI K. Effect of soldering condition on formation of intermetallic phases developed between Sn-0.3Ag-0.7Cu low-silver lead-free solder and Cu substrate [J]. Journal of Alloys and Compounds, 2011, 50: 6276−6279.

[4] ZHUA W J, WANG J, LIU H S, et al. The interfacial reaction between Sn-Ag alloys and Co substrate [J]. Materials Science and Engineering A, 2007, 456: 109−113.

[5] KIM K S, HUH S H, SUGANUMA K. Effects of intermetallic compounds on properties of Sn-Ag-Cu lead-free soldered joints [J]. Journal of Alloys and Compounds, 2003, 352: 226−236.

[6] YOON J W, JUNG S B. Reliability studies of Sn-9Zn/Cu solder joints with aging treatment [J]. Journal of Alloys and Compounds, 2006, 407: 141−149.

[7] CHUNG H M, CHEN C M, LIN C P, et al. Microstructural evolution of the Au-20wt%Sn solder on the Cu substrate during reflow [J]. Journal of Alloys and Compounds, 2009, 485: 219−224.

[8] LAI Y T, LIU C Y. Study of wetting reaction between eutectic AuSn and Au foil [J]. Journal of Electronic Materials, 2006, 35(1): 28−34.

[9] LEE K A, JIN Y M, SOHN Y H, et al. Continuous strip casting, microstructure and properties of Au-Sn soldering alloy [J]. Met Mater Int, 2011, 17(1): 7−14.

[10] TAN Q B, DENG C, MAO Y, et al. Evolution of primary phases and high-temperature compressive behaviors of as-cast AuSn20 alloys prepared by different solidification pathways [J]. Gold Bull, 2011, 44: 27−35.

[11] ERIKA H, MARIÁN P, EMIL L, et al. Kinetics of intermetallic phase formation at the interface of Sn-Ag-Cu-X (X=Bi, In) solders with Cu substrate [J]. Journal of Alloys and Compounds, 2011, 509: 7052−7059.

[12] HO C H, LIN S W, LIN Y C. Effects of Pd concentration on the interfacial reaction and mechanical reliability of the Sn-Pd/Ni system [J]. Journal of Alloys and Compounds, 2011, 509: 7749−7757.

[13] KUMAR A, CHEN Z. Influence of solid-state interfacial reactions on the tensile strength of Cu/electroless Ni-P/Sn-3.5Ag solder joint [J]. Materials Science and Engineering A, 2006, 423: 175−179.

[14] YOON J W, JUNG S B. Effect of surface finish on interfacial reactions of Cu/Sn-Ag-Cu/Cu (ENIG) sandwich solder joints [J]. Journal of Alloys and Compounds, 2008, 448: 177−184.

[15] MASSALSKI T B. Binary alloy phase diagrams [M]. Ohio: ASM International (Materials Park), 1990: 433.

[16] ANHOCK S, OPPERMANN H, KALLMAYER C, et al. Investigations of Au-Sn alloy on different end-metallizations for high temperature applications [C]// Proceedings of the 22nd IEEE/CPMT International Electronics Manufacturing Technology Symposium. Berlin, 1998: 156−165.

[17] LAURILA T, VUORINEN V, KIVILAHTI J K. Interfacial reactions between lead-free solders and common base materials [J]. Materials Science and Engineering R, 2005, 49: 1−60.

[18] BADER W. Dissolution of Au, Ag, Pd, Cu and Ni in a molten tin-lead solder [J]. Welding Journal, 1969, 48(12): 551−557.